Appl. Phys. B 89, 187–193 (2007)
DOI: 10.1007/s00340-007-2813-5

Applied Physics B
Lasers and Optics

K. SZYMANIEC[1,✉]
W. CHALUPCZAK[1]
S. WEYERS[2]
R. WYNANDS[2]

Prospects of operating a caesium fountain clock at zero collisional frequency shift

[1] National Physical Laboratory, Hampton Road, Teddington TW11 0LW, UK
[2] Physikalisch-Technische Bundesanstalt, Bundesallee 100, 38116 Braunschweig, Germany

Received: 14 June 2007/Revised version: 18 September 2007
Published online: 23 October 2007

ABSTRACT Recently it has been shown both theoretically and experimentally that, for certain operating conditions of a caesium fountain primary frequency standard, the cold-collision frequency shift, which can be a limit to the accuracy of the standard, strongly varies with the clock state composition and can be cancelled. This offers the intriguing prospect of operating a fountain standard at the zero-shift point, where no correction for collisions needs to be applied. We estimate expected improvements in the standard's accuracy and a potential shortening of the averaging time. Lastly, we derive relevant requirements for the key experimental parameters.

PACS 32.80.Pj; 06.20.-f

1 Introduction

Modern primary frequency standards (PFSs) use laser cooled atomic absorbers in a fountain configuration [1]. Atomic fountains are used not only in timekeeping applications but also in many fundamental physics tests where the highest experimental precision is needed. With the fountain approach long interrogation times and narrow velocity distributions have been achieved, which help to overcome many limitations of the earlier thermal beam standards. On the other hand, collisions between the atoms, which are usually negligible in beam standards, become a major issue: for laser-cooled atoms the de Broglie wavelength is much larger than the range of inter-atomic potentials. In particular, for the Cs atom, which is the basis of the SI definition of the second, the collision rate coefficients are large (compared to other alkalis) and also depend on collision energy in a non-trivial way [2]. The collisional frequency shift is one of the major factors limiting the accuracy of all caesium fountain frequency standards reported to date.

The usual method for evaluation of the collisional shift of a fountain based PFS is to operate the standard at different atom densities. This means that additional measurement time is needed to reach a specific statistical resolution. Several strategies have been implemented to find the best compromise between accuracy of the collisional-shift determination and clock instability (see, for instance [3, 4]). While the rate of frequency-shifting collisions is proportional to atom density, in practice one measures the total atom number in the cloud to scale and correct the collisional frequency shift. This method depends on the assumption that changes in the atom number do not result in changes in the spatial density distribution [5] (see also [6, 7]). The resulting uncertainty can be reduced by implementation of the adiabatic passage technique, which unambiguously links the density and the number of detected atoms [7], or by operating the fountain at very low densities [4]. The preferred solution would be to obviate or cancel the shift.

The possibility of cancellation of the collisional frequency shift has been considered previously [8]. Recently, it has been demonstrated experimentally [9] that there is an operating point for a fountain frequency standard where the collision-induced frequency shift vanishes (Fig. 1). This is due to the fact that the collisional shift cross-sections for the two clock states in Cs can have opposite signs and comparable absolute values. The experimental observations were supported by theoretical calculations based on precise values of the Cs scattering parameters [10] and a model of the expansion dynamics of the atomic cloud [11]. For a certain range of fountain parameters (specifically, of the initial radius ζ_0 and temperature T_0 of the atom cloud) the collisional frequency shift varies significantly when the composition of the clock states (set by the first Ramsey interaction) is varied. In particular, the collisional shift can be zero for a certain value of the clock state population ratio. Here, after recalling the idea of operating a fountain at zero collisional shift, we discuss in detail how the cancellation of the shift can shorten the required averaging time and hence improve the effective short-term stability of a fountain standard. Finally, we use the aforementioned model to estimate the residual frequency uncertainty when operating at (nominally) zero collisional shift for a set of realistic fountain parameters.

2 Variable collisional frequency shift

We start with a brief description of an atomic fountain caesium frequency standard (more details can be found in reviews such as [1]). Caesium atoms from a background

✉ Fax: +44 20 8943 6529, E-mail: ks1@npl.co.uk

vapour or a thermal beam are collected in a magneto-optical trap (MOT) or optical molasses. A cloud of about 10^7–10^8 atoms is formed, which has an approximately Gaussian distribution of density and atomic velocities. In the case of a MOT, the initial size ($e^{-1/2}$ radius) is typically $\zeta_0 \leq 1$ mm; in the case of a molasses the cloud is larger ($\zeta_0 = 3$–5 mm). The collection phase typically lasts up to about 0.5 s. Then the atoms are accelerated in a moving molasses and launched to an apogee some 80 cm above the cooling region. During the cooling and launching process the Cs atoms are optically pumped to the $|F = 4\rangle$ ground sublevel; afterwards atoms in $|F = 4, m_F = 0\rangle$ are selected and transferred to $|3, 0\rangle$ by a microwave pulse and those in $|F = 4, m_F \neq 0\rangle$ are removed by radiation pressure exerted by a laser pulse. The interrogation of the ground state hyperfine (clock) transition is performed using the Ramsey technique of separated fields. During the ballistic flight the atoms pass twice (on the way up and down) through a resonant microwave cavity installed approximately 30–40 cm below the apogee. After the second microwave interaction, the relative populations of the $|F = 3\rangle$ and $|F = 4\rangle$ states are detected by laser-induced fluorescence from which the transition probability is calculated. The number of detected atoms and their temperature can be extracted from this time-of-flight fluorescence signal. The observed Ramsey interference fringes typically have a full-width at half-maximum of $\Delta\nu \leq 1$ Hz, determined by the flight time between the two passages through the cavity. The contrast of the fringes can be almost 100% when the field amplitude in the cavity is adjusted such that during each passage the atoms experience a microwave pulse with an area (time-integrated Rabi frequency) of $\pi/2$. This corresponds to an equal weight of states $|3, 0\rangle$ and $|4, 0\rangle$ in the coherent superposition state prepared during the first Ramsey interaction.

In order to measure the frequency of the clock transition, the difference between the frequency ν of the local oscillator (LO) and the centre of the central Ramsey fringe ν_R is detected. In each fountain cycle the microwave frequency in the Ramsey cavity is toggled between $\nu + \Delta\nu/2$ and $\nu - \Delta\nu/2$. Thus the $|3, 0\rangle \rightarrow |4, 0\rangle$ transition probabilities are measured on either side of the central fringe and the difference $\nu - \nu_R$ is calculated from the imbalance in the measured probabilities.

The cold collisional frequency shift $\Delta\omega(E, t)$ is due to binary collisions at an instant t between the two Ramsey interactions. The shift depends on the collision energy $E = \frac{\mu}{2}(\boldsymbol{v}_1 - \boldsymbol{v}_2)^2$; μ is the reduced mass and $\boldsymbol{v}_1$ and $\boldsymbol{v}_2$ are the velocities of the colliding atoms. It can be written as

$$\Delta\omega(E, t) = \frac{1}{N}\langle[\lambda_{30}(E, t)\varrho_{30} + \lambda_{40}(E, t)\varrho_{40}] \times n(\boldsymbol{x}, \boldsymbol{v}_1, t)n(\boldsymbol{x}, \boldsymbol{v}_2, t)\rangle\,, \quad (1)$$

where $\langle\rangle$ denotes integration over spatial ($\boldsymbol{x}$) and velocity coordinates, $N = \langle n(\boldsymbol{x}, \boldsymbol{v}, t)\rangle$ is the total number of atoms, $n(\boldsymbol{x}, \boldsymbol{v}, t)$ is the density distribution of the cloud, λ_{30} (λ_{40}) and ϱ_{30} (ϱ_{40}) are the collision rate coefficient and the fractional population for the clock state $|3, 0\rangle$ ($|4, 0\rangle$). It is assumed that $|m_F \neq 0\rangle$ states are not populated and that $\varrho_{30} + \varrho_{40} = 1$. To find the collisional clock shift observed in the experiment the expression (1) has to be averaged over the time between the two Ramsey interactions. The shift varies linearly with the clock state composition parameterised, for example, by the ϱ_{40} population. For collision energies $E/k_B < 0.16\,\mu$K the collision rate coefficients λ_{30} and λ_{40} differ in sign [9]. Such low temperatures are easily reached in the atom cloud launched in a fountain: as a result of position-velocity correlations, which build up in a ballistically expanding cloud of atoms [12, 13], the effective collisional energy steadily decreases during its flight. Under suitable conditions it is possible to choose $\varrho_{40} = \varrho_{40}^{(C)}$ (via an adjustment of the microwave power in the Ramsey cavity) such that the overall accumulated collisional shift is zero (Fig. 1) [9].

The exact value of the zero-shift point $\varrho_{40}^{(C)}$ depends on the initial parameters of the atom cloud, ζ_0 and T_0, as well as on the timing of the Ramsey interactions [9]. For example, for $T_0 = 1\,\mu$K and a cloud size $\zeta_0 > 1$ mm, the collisional shift remains negative for all ϱ_{40}, excluding the possibility of cancellation. However, the typical size of a cloud of up to 10^8 atoms released from a MOT is about 0.5–0.7 mm and the expected $\varrho_{40}^{(C)} = 0.3$–0.4.

To evaluate the collisional frequency shift experimentally, a fountain is normally operated at two or more different atomic densities and the respective frequencies are measured against a stable reference (e.g., a hydrogen maser). The atom number (and density) is varied by, for example, varying the amplitude of the selecting microwave pulse. The evaluation of the collisional shift with an uncertainty below 10^{-15} may require averaging over about a day. Because the maser reference stability over this period may be poorer than the required resolution, it is convenient to alternate between atomic densities more frequently and to collect two separate sets of data, interlaced in time. The maser instabilities and any other common-mode frequency shifts are then rejected when calculating the frequency difference between the two sets of data.

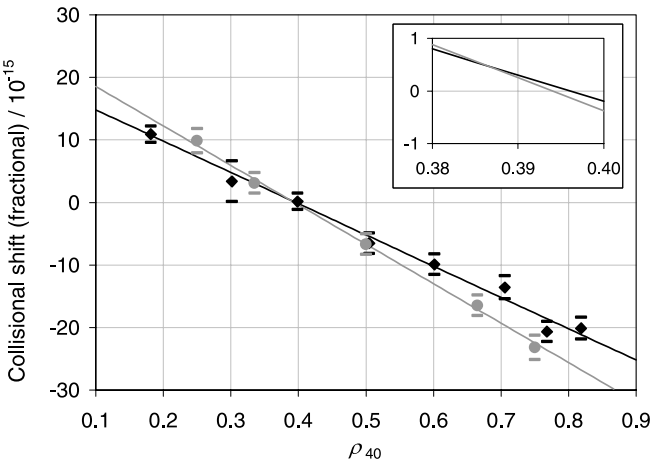

FIGURE 1 Illustration of the collisional shift variation and the cancellation point as a function of the fraction ϱ_{40} of atoms in $|4, 0\rangle$ after the first Ramsey interaction. Two sets of data taken with NPL-CsF1 are shown. The second measurement (*grey symbols*) was performed 6 months after the first one (*black symbols*). The steeper slope of the fit to the data indicated by *grey symbols* results from a higher atomic density. *Inset*: enlargement of the zero-crossing point. The cancellation point is $\varrho_{40}^{(C)} = 0.394$ and 0.396 for the two measurement campaigns, respectively. The residual collisional shift at $\varrho_{40}^{(C)}$ is stable to much better than 10^{-5} Hz (1 part in 10^{15}) as inferred from the fitted lines

3 Operation at the zero collisional shift point

The fractional clock state populations are set by the first interaction in the Ramsey cavity according to:

$$\varrho_{40} = 1 - \varrho_{30} = [\sin(x\pi/2)]^2 , \tag{2}$$

where x is a measure of the microwave field amplitude in the cavity (for a given Ramsey interaction time); $x = 0.5$ corresponds to $\pi/2$ pulses optimising the Ramsey fringe contrast in an idealized fountain. Although operating a fountain at $x \neq 0.5$ reduces the fringe contrast and therefore the signal-to-noise ratio, this effect can be minimised by applying $x = 0.5$ in the second interaction in the Ramsey cavity. It can be shown that in this case the contrast is reduced to $2p^{1/2}/(1+p)$, where p is the population ratio $\varrho_{40}/\varrho_{30} = [\tan(x\pi/2)]^2$ [8]. For example, for $\varrho_{40} = 0.4$ ($x = 0.44$) the contrast is reduced to 98% and even for $\varrho_{40} = 0.3$ ($x = 0.37$) only to 92%. Such minor losses of fringe contrast are outweighed by the potential gain in effective short-term stability following from the fact that the fountain PFS can be operated full-time under near-optimum operating conditions, without the need for auxiliary runs to take into account the collisional shift.

Let us consider a fountain operated alternately at high (optimum) and low densities n_{H} and n_{L} in order to determine the collisional-shift correction by extrapolating the frequency to zero density; $n_{\mathrm{H}}/n_{\mathrm{L}} = \kappa > 1$. For simplicity we assume that κ is known accurately. Possible inaccuracies of κ (not more than a few percent) do not affect the predictions presented here (see also [3]). The measured frequencies are ν_{H} and ν_{L}, and the extrapolated frequency ν_0 is given by

$$\nu_0 = (\kappa\nu_{\mathrm{L}} - \nu_{\mathrm{H}})/(\kappa - 1) . \tag{3}$$

The Allan deviation σ_{eff} of ν_0 is

$$(\kappa - 1)\sigma_{\mathrm{eff}}(2\tau) = \sqrt{\kappa^2\sigma_{\mathrm{L}}^2(\tau) + \sigma_{\mathrm{H}}^2(\tau)} , \tag{4}$$

where σ_{L} and σ_{H} are the Allan deviations for the fountain operating at low and high density, respectively, and τ is the averaging time for a single density (thus σ_{eff} is determined every 2τ). When the noise is dominated by the LO and the fountain cycle time T_{c} is kept unchanged between high and low density operation, $\sigma_{\mathrm{L}} \approx \sigma_{\mathrm{H}}$ and, for $\kappa = 2$,

$$\sigma_{\mathrm{eff}}(\tau) = \sqrt{2}\sigma_{\mathrm{eff}}(2\tau) = \sqrt{10}\sigma_{\mathrm{H}}(\tau) . \tag{5}$$

In the other limiting case, in which quantum projection noise (QPN) is dominant, the Allan standard deviation is inversely proportional to the square root of the detected atom number [14], thus $\sigma_{\mathrm{L}} = \sqrt{\kappa}\sigma_{\mathrm{H}}$ holds. Again, for $\kappa = 2$ and T_{c} unchanged:

$$\sigma_{\mathrm{eff}}(\tau) = \sqrt{18}\sigma_{\mathrm{H}}(\tau) . \tag{6}$$

In contrast, for operation at the zero-shift point (without extrapolation) the fountain could be run at optimum density n_{H} all the time, giving

$$\sigma_{\mathrm{eff}}(\tau) = \sigma_{\mathrm{H}}(\tau) . \tag{7}$$

The single Allan deviations for white frequency noise are proportional to $\tau^{-1/2}$, consequently, without density correction the measurement time to reach a specified statistical uncertainty $\sigma_{\mathrm{eff}}(\tau)$ is reduced by a factor of 10 or 18 with respect to the cases of (5) and (6). Additional time is needed beforehand to determine the zero shift point $\varrho_{40}^{(\mathrm{C})}$. In principle, this time could also be factored into $\sigma_{\mathrm{eff}}(\tau)$; since this would, however, make the effective stability dependent on the number of frequency points to be measured we opt here to treat that time separately (see Sect. 4 below).

We point out here that the value of the collisional shift correction might be affected by factors other than the atomic density (or the detected atom number). In Sect. 4.2 we discuss quantitatively the sensitivity of the collisional shift to launch parameters (ζ_0, T_0, initial velocity) and the field amplitude in the Ramsey cavity. In view of this discussion, a continually performed extrapolation to zero density appears as an adequate practice in operating a MOT-based fountain when the required long stability of the relevant parameters cannot be assured.

It has been suggested [15] that for the operation at the zero-shift point the atom density could still be alternated between n_{H} and n_{L}. A resulting differential measurement $\nu_{\mathrm{H}} - \nu_{\mathrm{L}}$ (nominally zero) could then provide a verification of the long-term stability of the fountain parameters relevant to the stability of the cancellation point (see Sect. 4.2). The frequencies ν_{H} and ν_{L} would be averaged in this case (rather than extrapolated), not causing any significant reduction in the effective stability, as long as $\sigma_{\mathrm{L}} \approx \sigma_{\mathrm{H}}$ holds.

Let us note that a reduction in averaging time can also be achieved for non-zero shift operation (e.g. the usual $\varrho_{40} = 0.5$) if the key requirement of the long-term stability of the fountain parameters is fulfilled. A one-to-one relation between the collisional shift and the detection signal needs to be established (instead of the $\varrho_{40}^{(\mathrm{C})}$ determination) and then used during the frequency measurement to apply the correction [6]. A disadvantage compared to the zero-shift operation is a systematic error due to an inaccuracy of that relation. Also the short-term stability is affected by fluctuations in the atomic density/atom number.

As the collisional shift cancellation can only be observed if the initial cloud size $\zeta_0 < 1$ mm (for temperatures $T_0 \approx 1\,\mu$K), for operation at zero collisional shift the maximum atom number in the MOT cloud cannot exceed approximately 10^8 [16], of which number about 10% end up in the $|3, 0\rangle$ state after state selection. Assuming that 20% of the selected atoms are detected after the Ramsey interaction, with a 1 Hz fringe width and a cycle time of 1 s, the corresponding short-term stability is $\sigma_{\mathrm{H}} = 0.3 \times 10^{-13}\,\tau(\tau/s)^{-1/2}$ if limited by QPN. In many cases, however, where the PFS uses a room temperature dielectric oscillator as a LO, the short-term stability is limited at about $\sigma_{\mathrm{H}} = 10^{-13}\,\tau^{-1/2}$ ($\sigma_0 = 3.2 \times 10^{-13}\,\tau^{-1/2}$) due to an aliasing effect (the so called Dick effect) [17] and very large atom numbers (large ζ_0) are not needed. For example, with a state-of-the-art BVA crystal [18] as LO, increasing the atom number in the MOT above 2×10^7 (about 2×10^6 atoms selected in $m_{\mathrm{F}} = 0$) has very little effect on the short-term stability. Note that the short-term stability of a PFS quoted in the literature often refers to σ_{H} rather than to σ_{eff}, which may be

larger by a significant factor (5) and (6). In that sense the shortening of the averaging time discussed here originates from a reduction of the effective short-term stability σ_{eff} (7).

4 Accuracy of the collisional shift evaluation

If a fountain operates at the compensated fractional population $\varrho_{40}^{(\mathrm{C})}$, the collisional frequency shift is nominally zero. However, there are two groups of factors contributing to the uncertainty of the collisional shift: the accuracy of the initial determination of $\varrho_{40}^{(\mathrm{C})}$ and the stability of its realisation during the fountain operation period. Using the theoretical model presented in [9, 11], we have analysed those factors in detail, aiming to estimate an uncertainty related to a residual collisional shift in a fountain operating at the zero-shift point. Unless stated otherwise, in the numerical examples following here, we consider a fountain with 2×10^7 atoms collected in a MOT (2×10^6 atoms selectively transferred to $|3,0\rangle$ and 4×10^5 detected) and of a short-term stability limited by LO noise at $\sigma_{\mathrm{H}}=\sigma_{\mathrm{L}}=10^{-13}$ (1 s). We further assume $T_0=1.5\,\mu\mathrm{K}$, $\zeta_0=0.55\,\mathrm{mm}$, launch height of 31 cm above the Ramsey cavity, which itself is positioned 54 cm above the MOT (as in the NPL fountain standard NPL-CsF1 [19]).

4.1 *Accuracy of the zero-shift point determination*

First we calculate the variable collisional shift as a function of ϱ_{40} for the parameters specified above. For the zero-shift point we obtain $\varrho_{40}^{(\mathrm{C})}=0.4$. In order to keep the residual collisional shift small ($<4\times10^{-16}$), $\varrho_{40}^{(\mathrm{C})}$ has to be determined with 2% accuracy. While the theoretical model reproduces the experimental data well [9], the accuracy of the $\varrho_{40}^{(\mathrm{C})}$ prediction is limited by the uncertainties in T_0 and ζ_0. Therefore in practice $\varrho_{40}^{(\mathrm{C})}$ has to be found experimentally. Moreover, the experimental determination may need to be repeated periodically owing to possible instabilities of the parameters affecting $\varrho_{40}^{(\mathrm{C})}$.

In principle, in order to find $\varrho_{40}^{(\mathrm{C})}$, one needs to obtain two points on the shift-versus-ϱ_{40} plot (Fig. 2). One method, which minimizes the measurement time, is to measure the collisional clock shift s_1 at one point and to extrapolate to zero using the slope

$$m=\frac{\Delta s}{\varrho_{40}^{(2)}-\varrho_{40}^{(1)}}\,, \tag{8}$$

of the linear dependence. The differential collisional shift Δs can be evaluated at low density, keeping in mind that $\sigma_{\mathrm{L}}=\sigma_{\mathrm{H}}$ in the LO noise limited case treated as an example here. The collisional clock shift is then

$$s_1=\nu_{\mathrm{L}}-\nu_0=(\nu_{\mathrm{H}}-\nu_{\mathrm{L}})/(\kappa-1)\,, \tag{9}$$

with ν_0 as in (3). For simplicity we will consider $\kappa=2$ in the following.

The zero-shift point is given by

$$\varrho_{40}^{(\mathrm{C})}=\varrho_{40}^{(1)}-\frac{s_1}{m}\,. \tag{10}$$

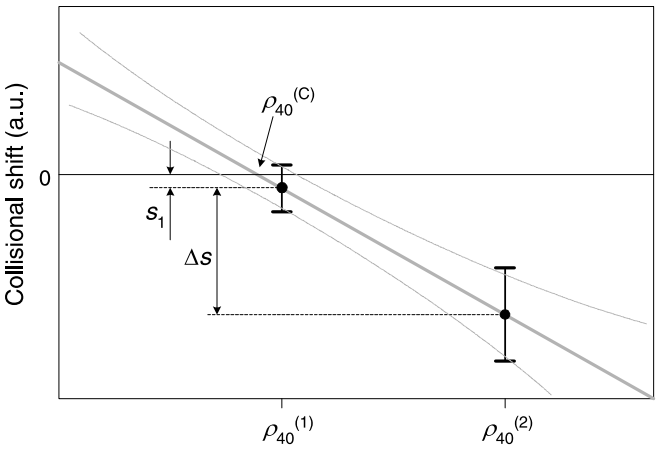

FIGURE 2 Procedure for the determination of the zero-shift point $\varrho_{40}^{(\mathrm{C})}$. The error bars for the point at $\varrho_{40}^{(1)}$ are equal to u_{s_1} and for the point at $\varrho_{40}^{(2)}$ are equal to $\sqrt{u_{s_1}^2+u_{\Delta s}^2}$

Experimentally, one needs to perform only three frequency measurements against a stable reference, possibly interlaced in time for common mode noise rejection: at $\varrho_{40}^{(\mathrm{I})}$ with high atomic density, at $\varrho_{40}^{(1)}$ with low density and at $\varrho_{40}^{(2)}$ with low density.

The residual clock shift u_{coll} (deviation from zero shift) related to an inaccurate determination of the zero-shift point $\varrho_{40}^{(\mathrm{C})}$ (with uncertainty $u_{\varrho\mathrm{C}}$) is given by:

$$u_{\mathrm{coll}}=m u_{\varrho\mathrm{C}}\,. \tag{11}$$

The values of $\varrho_{40}^{(1)}$ and $\varrho_{40}^{(2)}$ can be known sufficiently accurately that $u_{\varrho\mathrm{C}}$ (obtained from (10)) is dominated by the clock shift uncertainties u_{s_1} and $u_{\Delta s}$:

$$u_{\mathrm{coll}}=\sqrt{u_{s_1}^2+\left(\frac{s_1}{\Delta s}\right)^2 u_{\Delta s}^2}\,. \tag{12}$$

It is advantageous to choose $\varrho_{40}^{(1)}$ in the vicinity of the expected $\varrho_{40}^{(\mathrm{C})}$ value and $\varrho_{40}^{(2)}$ so that $s_1\ll\Delta s$. If u_{s_1} and $u_{\Delta s}$ are comparable, the residual collisional clock shift is then approximately $u_{\mathrm{coll}}\approx u_{s_1}$. In addition, any possible systematic error of s_1 due to nonlinearities in the dependence between the density and the detected atom number would be negligible as s_1 itself should be less than 10^{-5} Hz. For the example considered in this section,

$$u_{\mathrm{coll}}(3\tau)=\sqrt{\left(\frac{\sigma_{\mathrm{L}}(\tau)}{\beta}\right)^2+\left(\frac{\sigma_{\mathrm{H}}(\tau)}{\beta}\right)^2}=\frac{\sqrt{2}}{\beta}\sigma_{\mathrm{H}}(\tau) \tag{13}$$

and

$$u_{\mathrm{coll}}(\tau)=\sqrt{3}\cdot u_{\mathrm{coll}}(3\tau)=\frac{\sqrt{6}}{\beta}\sigma_{\mathrm{H}}(\tau)\,, \tag{14}$$

where τ is the averaging time required to achieve a given level of u_{coll}, β describes the reduction of the Ramsey fringe contrast (here $\beta=0.98$), and the factor $\sqrt{3}$ accounts for the three interlaced measurements, at $\varrho_{40}^{(1)}$ (n_{L} and n_{H}) and at $\varrho_{40}^{(2)}$, required to find s_1 and Δs.

The average time required to achieve $u_{\rm coll} \leq 10^{-15}$ ($\varrho_{40}^{(\rm C)}$ determination time) is approximately $\tau_{\rm determ} \approx 17\,{\rm h}$ (or 2.7 days for $u_{\rm coll} \leq 5 \times 10^{-16}$). After the initial determination of $\varrho_{40}^{(\rm C)}$, the fountain is expected to be operated without extrapolation of the collisional shift, providing a number of accurate frequency measurements over a period $\tau_{\rm oper}$, before the next determination of $\varrho_{40}^{(\rm C)}$ is required. The anticipated shortening of the averaging time in individual frequency measurements will only be realised if the determination of $\varrho_{40}^{(\rm C)}$ remains valid for $\tau_{\rm oper} \gg \tau_{\rm determ}$. In our example, $\tau_{\rm oper}$ would have to exceed several days or weeks, depending on the target residual statistical uncertainty u_0.

To measure p frequency points with the fountain clock to an uncertainty u_0 each (assuming white noise only) would therefore take the time

$$\tau_{\rm zero} = \left(\frac{6}{\beta^2} + p\right) \times \frac{\sigma_{\rm H}^2(1s)}{u_0^2} s\,, \tag{15}$$

in the case of operation at the zero-shift point and

$$\tau_{\rm extrapol} = 10p \times \frac{\sigma_{\rm H}^2(1s)}{u_0^2} s\,, \tag{16}$$

in the standard case of extrapolation to zero density. Even for $p = 1$, operation at the zero-shift condition is faster, with the advantage approaching an order of magnitude in time.

Let us add a remark about an alternative way of doing the density extrapolation, up to now the standard procedure employed in PTB-CSF1 [6]. Before and/or after each longer measurement period (typically $p > 15$) the fountain is run for several days with regularly alternating operation at high and low densities. From these additional runs the slope factor relating collisional shift and detected atom number is determined. This slope is then used off-line to correct all of the p points measured during the main campaign. This would result in (typically)

$$\tau_{\rm offline} = (10 + p) \times \frac{\sigma_{\rm H}^2(1s)}{u_0^2} s\,, \tag{17}$$

where the "10" above is the same as in (5) and (16). The difference to (15) appears relatively small but it should be borne in mind that the correction that has to be applied is rather large, so the demands on the stability of the experimental parameters are higher than for operation at the zero-shift point.

4.2 *Stability of the zero-shift point realisation*

As already indicated, the evolution of the effective collision energies in an expanding cloud (and hence the average clock shift) depends on the initial parameters ζ_0 and T_0. Therefore, the instability of these parameters over $\tau_{\rm oper}$ will limit the stability of $\varrho_{40}^{(\rm C)}$. Figure 3 shows average clock shifts calculated as a function of the initial cloud size for three initial temperatures. From the slope of the 1.5 μK curve (black solid line) we find that a 3% drift in the cloud size around $\zeta_0 = 0.55\,{\rm mm}$ results in a clock-shift variation of 4×10^{-16}.

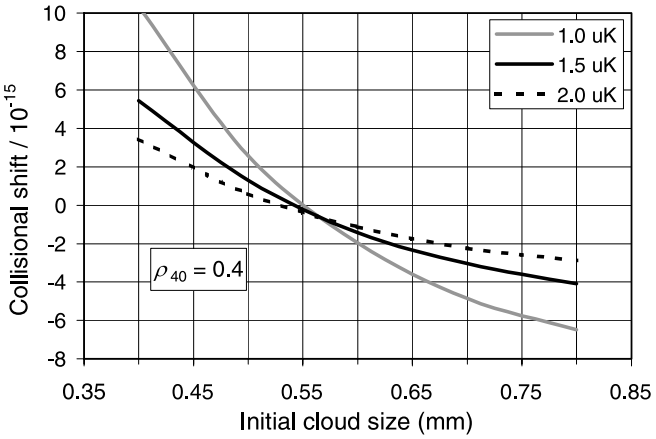

FIGURE 3 Collisional clock shift for a fixed fractional population $\varrho_{40} = 0.4$ as a function of the initial cloud size ζ_0 and three values of T_0 (1.0, 1.5, 2.0 μK); number of atoms at launch 2×10^7 (2×10^6 selected in $m_{\rm F} = 0$). The dependence of the shift on ζ_0 is stronger for lower temperatures. For the chosen range of T_0 one observes that at $\zeta_0 \approx 0.57$ the shift is almost independent of the launch temperature

Experimentally, the fluctuations and long-term drift in ζ_0 can easily be monitored during fountain operation. In Fig. 4 we show the Allan deviation of ζ_0, illustrating its short-term stability. For averaging times longer than 10–20 s the values are about 1% and almost constant, which indicates that a $1/f$ noise process is dominant. Currently we do not have enough data for a direct demonstration of the long-term stability of ζ_0. Indirectly, the long-term stability can be inferred from the inset of Fig. 1, indicating that the residual clock shift can remain in the 10^{-16} range for many months. Furthermore, it is possible to introduce a number of improvements in the experimental set-up (e.g. magnetic shielding of the trapping region, active stabilisation of amplitude and polarisation of the cooling beams) in order to reduce the fluctuations of ζ_0.

The sensitivity of the clock shift to fluctuations of T_0 is presented in Fig. 5. For various ζ_0 we calculate the corresponding $\varrho_{40}^{(\rm C)}$ values. For each ζ_0 we then calculated the expected residual clock shifts due to a 10% change of T_0 (0.15 μK). The 10% value is a conservative estimate of the

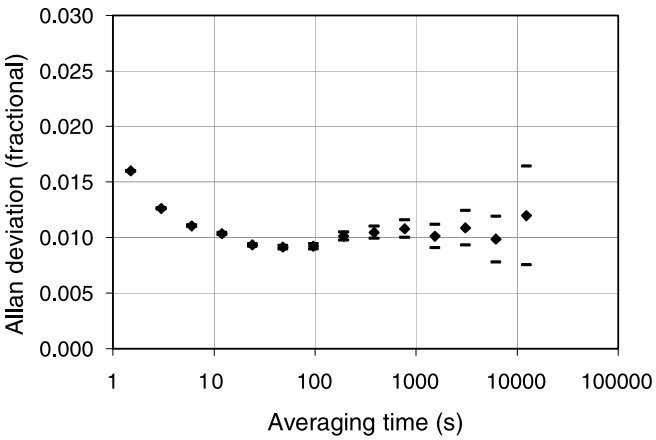

FIGURE 4 Allan deviation of the cloud size measured during the molasses phase before the launch in NPL-CsF2. The deviation levels off at about 1% value, suggesting that the noise process is predominantly of $1/f$ type

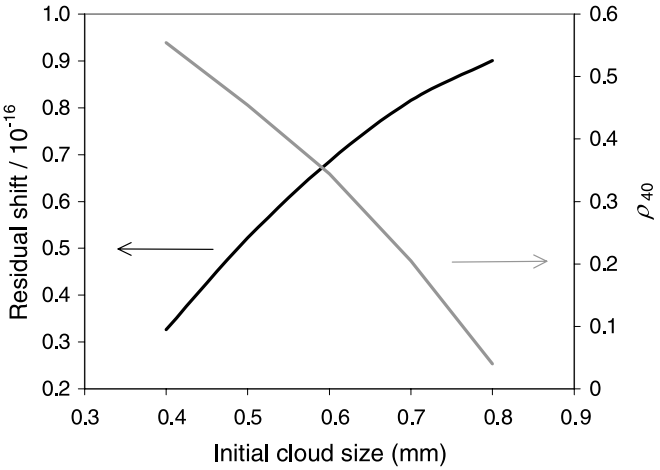

FIGURE 5 Residual collisional clock shift in the vicinity of the zero-shift point for a 10% variation in T_0. In the first step, as a function of ζ_0 the respective values of $\varrho_{40}^{(C)}$ are calculated for $T_0 = 1.5\,\mu$K (*grey line*, *right vertical axis*). In the second step, the residual shift (*black line*, *left vertical axis*) is calculated for each ζ_0 for these values of $\varrho_{40}^{(C)}$, but for a slightly changed temperature of $T_0 = 1.35\,\mu$K

temperature fluctuations in a fountain experiment. We also note that there is some correlation between changes in ζ_0 and the clock shift sensitivity to changes in temperature (Fig. 3). Taking this into account we obtain a residual shift smaller than 10^{-16}, if T_0 is stable to 10% (and ζ_0 to 3%).

Our theoretical model also allows us to search for the bounds of the collisional shift variations due to instability of the microwave field amplitude in the Ramsey cavity, which defines the fractional population ϱ_{40}. In order to keep the shift uncertainty at 10^{-16} or less, ϱ_{40} must be stable to 1% or better and the microwave field amplitude (parameter x) to 0.6%. While a microwave source output can achieve such stability, the coupling efficiency of the microwaves to the cavity also depends on the cavity detuning. For example, for a cavity Q-value of 10^4 the 0.6% stability in x requires the tuning to be stable within 60 kHz if the cavity is tuned to the atomic resonance. This is equivalent to a cavity temperature stability of about 0.3 K, well within the range of a simple temperature servo.

As mentioned in Sect. 2, the collisional shift observed in the experiment is the time average of the instantaneous shift between the instants of the two Ramsey interactions. In Fig. 6 we have shown the effective instantaneous shift, weighted by the decreasing atom number density, as a function of flight time. Any variation in the launch height (i.e. the averaging period for the instantaneous collisional shift) would result in a variation of the observed overall collisional shift. This effect is shown in Fig. 7. We find that such variations would be of the order of 0.5×10^{-16} if the launch height were stable to 2 mm (inset of Fig. 7). By measuring the time-of-flight to the detection region one can monitor possible fluctuations of the launch height and the required stability is normally achieved in the experiment.

We stress that if a MOT-based fountain is to be operated without the continuous extrapolation to zero density, either at the zero-shift point or at any other value of ϱ_{40}, it is necessary to analyse and maintain the required stability of the relevant parameters over the measurement period.

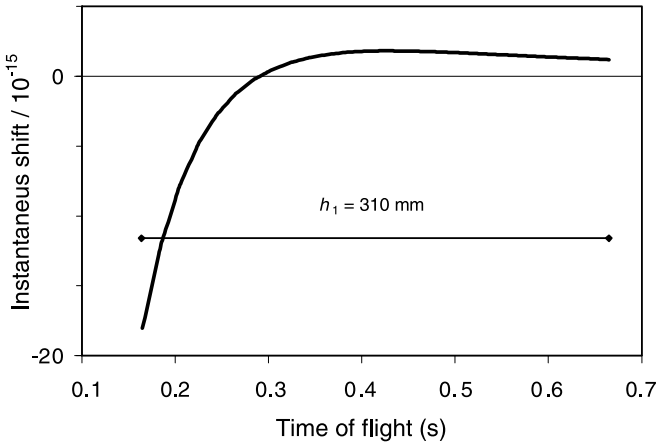

FIGURE 6 Instantaneous collisional shift calculated according to formula (1); $\varrho_{40} = 0.4$. The time of the Ramsey interaction for a launch height of 31 cm (above the cavity centre) is indicated

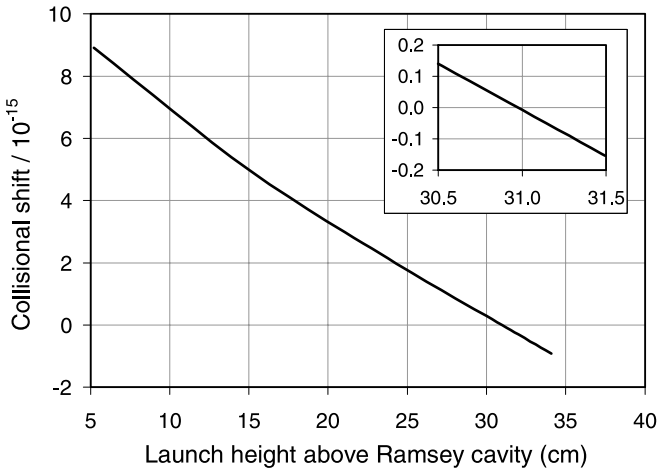

FIGURE 7 Predicted collisional frequency shift as a function of launch height. The microwave cavity position is 54 cm above the MOT; other parameters are: $\zeta_0 = 0.55$ mm, $T_0 = 1.5\,\mu$K, $\varrho_{40} = 0.4$, and the number of $m_F = 0$ selected atoms 2×10^6. *Inset*: variations of the shift in the vicinity of the nominal launch height for the NPL-CsF1 fountain (31 cm)

The accuracy of the collisional shift evaluation for a fountain operating at $x \neq 0.5$ (required for $\varrho_{40} = \varrho_{40}^{(C)}$), might be affected by the effect of cavity pulling, which also causes a frequency shift proportional to the number of atoms (first-order effect) [20, 21]. We estimate that in the case discussed above (2×10^6 atoms in a cavity tuned to resonance) this effect is small ($< 10^{-16}$). Also the second-order pulling effect, independent of the atom number [22], is negligible despite operating at $x \neq 0.5$.

Finally we point out that the ultimate limit of the collisional shift evaluation, in the non-extrapolating as well as in the extrapolating mode, is related to collisions with atoms populating $|F = 3, m_F \neq 0\rangle$ (e.g., due to optical pumping by the radiation pressure pulse after the state selection) [23]. Again, the effect is expected to be negligible for the number of atoms in the fountain considered in our example.

5 Conclusions

We have shown that it should be possible to operate a MOT-based fountain frequency standard without having to

Parameter	Permissible instability	Residual shift (fractional)
Initial cloud size, ζ_0	3%	4×10^{-16}
Temperature at launch, T_0	10%	1×10^{-16}
Microwave field amplitude, x	0.6%	1×10^{-16}
(cavity temperature, T_{cav})	(0.3 K)	
Launch height	2 mm	0.5×10^{-16}

TABLE 1 Summary of the stability requirements for the key fountain parameters and their effect on the residual collisional shift at $\varrho_{40}^{(\mathrm{C})}$

apply any corrections for cold collisions. When operating the standard at the zero collisional shift point the extrapolation to zero density would not be needed and the residual clock shift should not exceed parts in 10^{16} (Table 1). The related type-B uncertainty of the collisional shift would be dominated by the statistical resolution of the $\varrho_{40}^{(\mathrm{C})}$ determination (averaging time τ_{determ}) and the long-term stability of ζ_0. The stability of T_0 is less critical. Similarly, the stability of the microwave field amplitude seen by the atoms can be achieved at the required level, provided the Ramsey cavity is temperature stabilised. Such operation of the fountain standard may require some additional experimental effort but in return it offers a much improved effective short-term stability and about a ten-fold reduction in averaging time. In this way the performance of the relatively simple fountain PFS, based on a single stage MOT and a room temperature LO, comes closer to that which, to date, has been achieved only in standards using sophisticated multi-stage cold atom sources and cryogenically cooled oscillators. A possible differential measurement by alternating the operational density could also increase one's confidence in the continued stability of the zero-shift operation. Lastly, even if the required stability of the parameters were impossible to achieve in a particular realisation of a fountain standard, operation at $\varrho_{40}^{(\mathrm{C})}$ with extrapolation to zero density would still help to reduce the systematic uncertainty of the collisional shift, often approximately proportional to the shift itself [6].

Our analyses are based on the modelling of the dynamics of the atom cloud. We stress that the conditions for the collisional shift cancellation depend strongly on the initial cloud parameters and timing of the Ramsey interaction. Therefore the numerical estimates presented in this paper cannot be applied to other experimental realisations directly, although the general conclusions presented here remain valid. Furthermore, any experiments performed with fountain clocks that involve altered cloud dynamics will need to be carefully evaluated to make sure that the concomitant change of the overall collisional shift does not impact the result of the experiment. For instance, experiments using a variable toss height [24] could be affected because the effective temperature and therefore the effective collisional cross-section depend on the flight time of the cloud. Similarly, if the fractional populations of the clock states are inadvertently altered, for example in a test operation at elevated microwave power, an apparent frequency shift may be observed [25]. We also point out that the use of a small atom cloud, which is essential for the collisional shift cancellation, may entail an increase of other systematic effects in fountain primary frequency standards (for example, frequency shifts due to cavity phase gradients [26, 27] or an increased sensitivity to microwave leakage due to the stronger expansion of a smaller cloud [28]).

ACKNOWLEDGEMENTS The authors would like to thank Stephen N. Lea for useful comments on the manuscript. The NPL authors acknowledge support from the Pathfinder Programme of the UK National Measurement System.

REFERENCES

1 R. Wynands, S. Weyers, Metrologia **42**, S64 (2005)
2 P. Leo, P.S. Julienne, F.H. Mies, C.J. Williams, Phys. Rev. Lett. **86**, 3743 (2001)
3 F. Levi, D. Calonico, L. Lorini, A. Godone, Metrologia **43**, 545 (2006)
4 T.P. Heavner, S.R. Jefferts, E.A. Donley, J.H. Shirley, T.E. Parker, Metrologia **42**, 411 (2005)
5 K. Gibble, S. Chu, Phys. Rev. Lett. **70**, 1771 (1993)
6 S. Weyers, A. Bauch, R. Schroeder, C. Tamm, Proc. 6th Symp. on Frequency Standards and Metrology, ed. by P. Gill (World Scientific, Singapore, 2002), p. 64
7 F. Pereira Dos Santos, H. Marion, S. Bize, Y. Sortais, A. Clairon, C. Salomon, Phys. Rev. Lett. **89**, 233 004 (2002)
8 K. Gibble, B.J. Verhaar, Phys. Rev. A **52**, 3370 (1995)
9 K. Szymaniec, W. Chalupczak, E. Tiesinga, C.J. Williams, S. Weyers, R. Wynands, Phys. Rev. Lett. **98**, 153 002 (2007)
10 C. Chin, V. Vuletic, A.J. Kerman, S. Chu, E. Tiesinga, P.J. Leo, C.J. Williams, Phys. Rev. A **70**, 032 701 (2004)
11 W. Chalupczak, K. Szymaniec, J. Phys. B **40**, 343 (2007)
12 K. Gibble, S. Chang, R. Legere, Phys. Rev. Lett. **75**, 2666 (1995)
13 V. Venturi, E. Tiesinga, C.J. Williams, (unpublished)
14 G. Santarelli, P. Laurent, P. Lemonde, A. Clairon, A.G. Mann, S. Chang, A.N. Luiten, C. Salomon, Phys. Rev. Lett. **82**, 4619 (1999)
15 K. Gibble, private communication
16 C.G. Townsend, N.H. Edwards, C.J. Cooper, K.P. Zetie, C.J. Foot, A.M. Steane, P. Szriftgiser, H. Perrin, J. Dalibard, Phys. Rev. A **52**, 1423 (1995)
17 G. Santarelli, C. Audoin, A. Makdissi, P. Laurent, G.J. Dick, A. Clairon, IEEE Trans. Ultrason. Ferroelectr. Freq. Control **45**, 887 (1998)
18 P. Laurent, M. Abgrall, C. Jentsch, P. Lemonde, G. Santarelli, A. Clairon, I. Maksimovic, S. Bize, C. Salomon, D. Blonde, J.F. Vega, O. Grosjean, F. Picard, M. Saccoccio, M. Chaubet, N. Ladiette, L. Guillet, I. Zenone, C. Delaroche, C. Sirmain, Appl. Phys. B **84**, 683 (2004)
19 K. Szymaniec, W. Chalupczak, P.B. Whibberley, S.N. Lea, D. Henderson, Metrologia **42**, 49 (2005)
20 C. Fertig, K. Gibble, Phys. Rev. Lett. **85**, 1622 (2000)
21 S. Bize, Y. Sortais, C. Mandache, A. Clairon, C. Salomon, IEEE Trans. Instrum. Meas. **50**, 503 (2001)
22 J. Vanier, C. Audoin, *The Quantum Physics of Atomic Frequency Standards* (Adam Hilger, Bristol, Philadelphia, 1989), p. 830
23 H. Marion, S. Bize, L. Cacciapuoti, D. Chambon, F. Pereira dos Santos, G. Santarelli, P. Wolf, A. Clairon, Proc. 18th European Frequency and Time Forum (2004)
24 F. Levi, A. Godone, L. Lorini, IEEE Trans. Ultrason. Ferroelectr. Freq. Control **48**, 847 (2001)
25 K. Szymaniec, W. Chalupczak, S. Weyers, R. Wynands, IEEE Trans. Ultrason. Ferroelectr. Freq. Control **54**, 1721 (2007)
26 R. Li, K. Gibble, Metrologia **41**, 376 (2004)
27 S.R. Jefferts, J.H. Shirley, N. Ashby, E.A. Burt, G.J. Dick, IEEE Trans. Ultrason. Ferroelectr. Freq. Control **52**, 2314 (2005)
28 S. Weyers, R. Schroeder, R. Wynands, Proc. 20th European Frequency and Time Forum (2006), p. 173